

Arc statistics with realistic cluster models

Massimo Meneghetti

*Dipartimento di Astronomia, Università di Padova, Vicolo
dell'Osservatorio 2, I-35122, Padova, Italy*

Matthias Bartelmann

*Max-Planck-Institut für Astrophysics, Karl-Schwarzschild-Strasse 1,
D-85748 Garching, Germany*

Lauro Moscardini

*Dipartimento di Astronomia, Università di Bologna, Via Ranzani 1,
I-40127, Bologna, Italy*

Elena Rasia

*Dipartimento di Astronomia, Università di Padova, Vicolo
dell'Osservatorio 2, I-35122, Padova, Italy*

Giuseppe Tormen

*Dipartimento di Astronomia, Università di Padova, Vicolo
dell'Osservatorio 2, I-35122, Padova, Italy*

Elena Torri

*Dipartimento di Astronomia, Università di Padova, Vicolo
dell'Osservatorio 2, I-35122, Padova, Italy*

Abstract. Arc statistics is known to be a powerful cosmological tool. Numerical lensing simulations show that orders of magnitude differences in the number of *giant* arcs on the whole sky are expected in different cosmological models. In this paper, we discuss the analytic and numerical methods in arc statistics and show that analytic models fail to reproduce the efficiency for strong lensing of more realistic numerical cluster models. Then, we discuss two recent extensions of the lensing simulations, i.e. the effects of cD galaxies in the lensing clusters and the impact of cluster mergers on arc statistics. We show that cD galaxies can increase the lensing cross sections for long and thin arcs by perhaps up to $\sim 50\%$, while major mergers can change the cluster efficiency for producing such arcs by up to one order of magnitude.

1. Introduction

Many factors determine the abundance of strong lensing events, i.e. gravitational arcs, in galaxy clusters. Very shortly, since the light deflection depends on the distances between observer, lens and source, gravitational lensing depends on the geometrical properties of the Universe. Moreover, gravitational arcs are rare events caused by a highly nonlinear effect in cluster cores, and are thus not only sensitive to the number density of galaxy clusters, but also to their internal structure.

Since all of these factors depend on cosmology, the statistical study of strong gravitational lensing events in galaxy clusters is a powerful cosmological tool. In particular, we expect that arc statistics is very sensitive to the values of Ω_0 and Ω_Λ . Indeed, the expected number of *giant* arcs, usually defined as arcs with a length-to-width ratio exceeding ten and apparent B -magnitude less than 22.5 (Wu & Hammer, 1993), changes by orders of magnitude between low- and high-density universes according to the numerical models described in Bartelmann et al. (1998).

In the next sections of this paper, we discuss the possible methods for constraining the cosmological parameters using arc statistics and we consider some extensions of the previous studies, modeling in as much detail as possible some of the effects that may influence or distort the conclusions drawn from the morphology and number of gravitationally lensed arcs.

2. Numerical vs. Analytic methods

Two approaches have been followed in arc statistics studies so far. The first is based on numerical methods: the ray-tracing technique is used for studying the lensing properties of clusters taken from N-body simulations. This allows the most realistic description of the cluster lenses because all effects which could play an important role in the lensing phenomena (like asymmetries, substructures in the mass distribution, etc.) are by construction taken into account. However, given the long computation times required for full numerical simulations of cluster lensing, it is currently not feasible to perform such simulations for sufficiently many combinations of the essential cosmological parameters, i.e. the matter density parameter Ω_0 and the cosmological constant Ω_Λ .

In a conceptually different approach, simple analytic, axially symmetric models have been used for describing the density profiles of cluster lenses. This method of investigation has the advantage that the computation of the probability for arcs satisfying a specified property is fast and can easily be performed for a continuous and wide range of cosmological parameters, because the lensing properties of these models are perfectly known and fully described by analytic formulae. However they give a less realistic description of cluster lenses.

The correspondence between analytic and numerical models remains unclear. While the analytic studies by Cooray et al. (1999) and Kaufmann & Straumann (2000) find similar results as the numerical simulations regarding the sensitivity of arc statistics to the cosmic density parameter, their results are almost insensitive to the cosmological constant, in marked contrast to the previously mentioned results by Bartelmann et al. (1998), who found order-of-

magnitude changes in the expected number of giant arcs between low-density models with and without a cosmological constant.

In order to check the consistency of the analytic and numerical methods in arc statistics, we perform a comparative study of lensing cross sections of numerical cluster models and several their analytical approximations. We summarize here our main results referring the reader to the paper by Meneghetti, Bartelmann & Moscardini (2003a) for a more detailed discussion.

2.1. Axially symmetric models

Previous analytic studies of arc statistics commonly used the Singular Isothermal Sphere (SIS hereafter) model for describing cluster lenses. The density profile of this model is given by

$$\rho(r) = \frac{\sigma_v}{2\pi G r^2}, \quad (1)$$

where σ_v is the velocity dispersion and r is the distance from the sphere center.

This model is computationally convenient, but has an unrealistic density profile for clusters. Indeed, several observations, for example the occurrence of radial arcs in some galaxy clusters, indicate that cluster density profiles are far from isothermal. Navarro, Frenk & White (1997) (NFW hereafter) found that the density profile of dark matter halos numerically simulated in the framework of CDM cosmogony can be very well described by the radial function

$$\rho(r) = \frac{\rho_s}{(r/r_s)(1 + r/r_s)^2}, \quad (2)$$

within the wide mass range $3 \times 10^{11} \lesssim M_{\text{vir}}/(h^{-1}M_{\odot}) \lesssim 3 \times 10^{15}$. The logarithmic slope of this density profile changes from -1 at the center to -3 at large radii. Therefore, it is flatter than that of the SIS in the inner part of the halo, and steeper in the outer part. The two parameters r_s and ρ_s are the scale radius and the characteristic density of the halo. They are not independent and can thus be expressed in terms of the halo virial mass, which is in fact the only free parameter.

An important feature of this model is that it reflects the theoretically expected dependence of halo concentration, defined as the ratio of the virial and scale radius, $c = r_{\text{vir}}/r_s$, on cosmology. Halos are the more concentrated the earlier they form and this important property is reproduced by the NFW model.

Several different aspects of lensing by halos with NFW or generalized NFW profiles can be found in Bartelmann (1996), Wright & Brainerd (2000), Li & Ostriker (2002), Wyithe, Turner & Spergel (2001), Perrotta et al. (2001), Meneghetti et al. (2003a), Bartelmann et al. (2002a, 2002b). We refer the reader to those papers for more details.

2.2. Elliptical model

The construction of lens models with elliptical or pseudo-elliptical isodensity contours is generally quite complicated (Kassiola & Kovner, 1992; Kormann et al., 1994; Golse & Kneib, 2002). Obtaining the potential corresponding to these kinds of density distributions can become extremely complicated, even for quite simple lens models. It is simpler and often sufficient to model a lens by means of an elliptical effective lensing potential.

For any axially symmetric lensing potential in the form

$$\Psi(x) = f(x) \quad (3)$$

we can obtain its elliptical generalization by substituting

$$x \rightarrow X = \sqrt{\frac{x_1^2}{(1-e)} + x_2^2(1-e)}, \quad (4)$$

where $e = 1 - b/a$ is the ellipticity and a and b are the major and minor axis of the ellipse. This ensures that the mass inside circles of fixed radius remains constant as the ellipticity changes.

2.3. Numerical models

We analyze the lensing properties of five numerically simulated cluster-sized dark-matter haloes, kindly made available by the GIF collaboration (Kaufmann et al., 1999). They were obtained from N -body simulations performed in the framework of three different cosmological models. These are an Einstein-de Sitter model (hereafter SCDM); a flat, low-density universe with a matter density parameter $\Omega_0 = 0.3$ and a cosmological constant $\Omega_\Lambda = 0.7$ (Λ CDM); and an open, low-density model with $\Omega_0 = 0.3$ and $\Omega_\Lambda = 0$ (OCDM). The virial masses of the clusters at redshift $z = 0$ range between $\sim 5 \times 10^{14} M_\odot/h$ and $\sim 2 \times 10^{15} M_\odot/h$. For each of these clusters, we took several simulation snapshots at different epochs, between $z = 0$ and $z = 1$.

The lensing properties of these clusters are studied using a ray-shooting technique (Bartelmann et al., 1998, Meneghetti et al., 2000, Meneghetti et al., 2001, Meneghetti et al., 2003a). By projecting the numerically simulated clusters along the line of sight, we obtain surface density maps, which we use as lens planes in the lensing simulations. A bundle of 2048×2048 light rays is then traced through the mass distributions and their deflection angles are computed by summing up the contribution from each mass element of the deflector. We finally reconstruct the images of a large number of background elliptical sources, placed at redshift $z_s = 1$. It results in a catalogue of simulated images which is subsequently analyzed statistically.

2.4. Lensing cross sections

The lens efficiency for producing arcs with a given property is quantified by the lensing cross section. By definition, it is the area on the source plane where a source must be placed in order to be imaged as an image with the specified property.

For axially symmetric lenses, the lensing cross section can be computed analytically or semi-analytically. For more complex lens models, like the numerically simulated clusters or the pseudo-elliptical NFW model, numerical techniques are required (e.g. see Meneghetti et al., 2003a).

We focus here on long and thin arcs, i.e. arcs with a length-to-width ratio L/W larger than a minimal threshold. As anticipated earlier, we compare the lensing cross sections for this kind of arcs of the numerical and analytic models introduced in the previous sections. For clarity, we present here the results

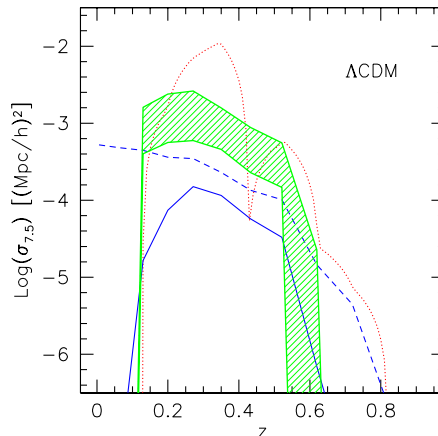


Figure 1. Lensing cross sections for arcs with length-to-width ratio larger than 7.5 as a function of the lens redshift. See text for more details.

obtained for the most massive halo only. The behavior of the cross sections for the other numerical models is in good qualitative and quantitative agreement with that obtained for this cluster.

The results are illustrated in Fig. (1), where the dotted line refers to the fully numerically simulated cluster, while solid and dashed lines represent the cross sections of NFW and SIS lenses, respectively, having the same virial mass as the numerical cluster model. Finally, the shaded region in the same plot shows the cross sections obtained by elliptically distorting the NFW lensing potential with ellipticities e in the range between $e = 0.2$ and $e = 0.4$ (lower and upper limits, respectively). Results are shown for $L/W \geq 7.5$ and they were obtained for the Λ CDM model. Consistent results were found in the other investigated cosmological models and for other minimal L/W ratios.

The general trends in the lensing cross sections shown in Fig. (1) can be understood as follows. The strong-lensing efficiency of a mass distribution depends on several factors. First, for the light coming from the sources to be focused on the observer, the lens must be located at a suitable distance from both the observer and the sources. Second, the larger the (virial) mass of the lens is, the stronger are the lensing effects it produces close to its center. Finally, the more concentrated the lens is, the thinner are the long arcs expected to be. Since the lens mass grows with decreasing redshift because new material is accreted by the halo and deepens its potential well, the lensing cross sections are expected to grow as well. On the other hand, when the lens is too close to the observer, the cross section is geometrically suppressed, unless the lens surface density profile is sufficiently steep and scale-free, as for the SIS lenses. In fact, in this case the focusing by the lens is strong enough to allow observers to see strongly distorted images of background sources also in very near lenses, i.e. at relatively small redshifts.

The numerical models generally have much larger cross sections than the analytic models. In particular, the cross sections for axially symmetric NFW

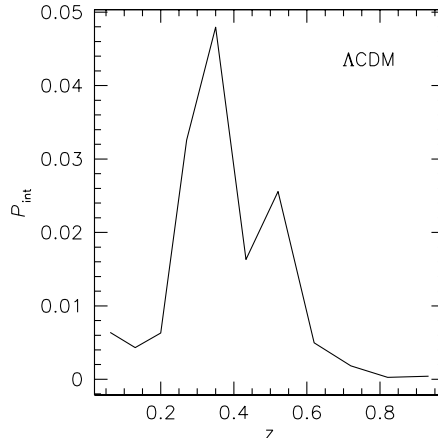


Figure 2. Integrated multipole power as a function of redshift for the most massive cluster in our numerically simulated sample.

lenses are almost two orders of magnitude smaller. For SIS lenses, the discrepancy with the numerical models is only partially compensated by the unrealistically steep central density profile, but the estimated values of $\sigma_{7.5}$ remain too low. Introducing the elliptical distortion into the NFW lens model allows the cross section to increase by roughly an order of magnitude compared to the axially symmetric NFW model, but even then the analytic cross sections fail to reproduce the numerical cross sections unless unrealistically high values of e are adopted.

Since the ellipticity of the mass distribution alone cannot fully explain the discrepancy between numerical and analytic models, the remaining difference must be attributed to some factors which are missing from the analytical models. The most important of those is certainly the presence of substructure in the lensing mass distribution.

Deviations of the projected mass distribution of a numerically simulated cluster from the predictions of circular or elliptical models can be quantified by means of a multipole expansion of its surface density field (see Meneghetti et al., 2003a). By integrating the power spectrum of this multipole expansion and by subtracting the contributions from the monopole and the quadrupole, we build up a quantity, \bar{P}_{int} , which directly measures the amount of substructures and the degree of asymmetry in the mass distribution of the lens.

In Fig. (2) we show how the integrated power \bar{P}_{int} averaged within the virial radius of the cluster changes as a function of the cluster redshift for the lens whose cross section was plotted in Fig. (1). For better comparing the dependences on redshift of the integrated power and the lensing cross sections, we have rescaled \bar{P}_{int} with the effective lensing distance and with the virial cluster mass. A quick comparison of this curve to the lensing cross sections in Fig. (1) shows that the redshifts where the contributions of the dipole and the higher-order multipoles are largest correspond quite well to those where the numerical cross sections deviate most strongly from those of the elliptical models.

3. The arc statistics problem

In the previous section we showed that reliable predictions of arc cross sections require realistic cluster models, i.e. numerically simulated clusters. As anticipated earlier, by investigating the lensing properties of a sample of clusters obtained from N-body simulations in the framework of several cosmological models, Bartelmann et al. (1998) found orders of magnitude differences between the number of giant arcs which are expected to be seen on the whole sky in different cosmological models. In particular, they estimated that ~ 3000 giant arcs would be produced in a Λ CDM model, while one order of magnitude less arcs are expected in a Λ CDM model.

Observations of the abundance of gravitational arcs in galaxy clusters seem to be consistent only with the predictions for an open universe (Luppino et al., 1999; Zaritsky et al., 2002; Gladders et al., 2003). This is in pronounced disagreement with other observational results, in particular those obtained from the recent experiments on the cosmic microwave background (de Bernardis et al., 2000; Bennett et al., 2003) and the observations of high-redshift type-Ia supernovae (Perlmutter et al., 1998), which all suggest instead that the cosmological model most favored by the data is spatially flat and dominated by a cosmological constant. This is known as the *arc statistics problem*.

Several extensions and improvements of the numerical simulations failed in finding a solution to this problem in the lensing simulations. For example, Meneghetti et al. (2000) studied the influence of individual cluster galaxies on the ability of clusters to form large gravitational arcs, finding that their effect is statistically negligible.

In the next sections we discuss whether the presence of a central cD galaxy or the occurrence of mergers in the lensing clusters can alter the conclusions of previous arc statistics studies and solve the arc statistics problem.

3.1. Effects of cD galaxies on arc statistics

The centers of massive galaxy clusters are generally dominated by very massive ($\sim 10^{13} M_{\odot}$) cD galaxies, which could in principle noticeably affect the strong-lensing properties of their host clusters. In fact, due to their more concentrated dark matter halos, they may steepen the inner slope of the cluster density profile and push the cluster critical curves to larger distances from the center. Thus, the length of the critical curves may be increased, and thus the probability for long arcs to form. Moreover, cD galaxies may help their host clusters to reach the critical central surface density for producing critical curves and becoming efficient strong lenses.

For investigating the effects of cD galaxies on arc statistics, we study the lensing properties of the same sample of five numerically simulated galaxy clusters described in Sect. 2.3, restricting our analysis to the Λ CDM and the Λ CDM cosmological models (Meneghetti, Bartelmann & Moscardini, 2003b). We measure their efficiency for producing tangential and radial arcs before and after the inclusion of a cD galaxy. The central galaxy is modeled using both the axially symmetric and elliptical models discussed in Sect. 2.1 and 2.2 and assuming a range of virial masses and possible orientations with respect to the mass distribution of the host cluster.

The inclusion of the cD galaxy in the cluster lens has been done as follows. Being linear function of mass, the total deflection angle of a ray passing through a mass distribution is the sum of the contributions from each mass element of the deflector. Therefore, in the case of a galaxy cluster, we can decompose the cluster lens into its smoothed dark matter component, plus the granular component contributed by its galaxy population (see also Meneghetti et al. 2000). For both the cluster and the galaxies, the main constituent is given by the dark matter which forms their halos. Our model of the cluster containing a cD galaxy can thus be fairly simple; we take the smoothed dark matter distribution obtained from the numerical simulations described above, and introduce a dark-matter halo resembling the galaxy. For each ray traced through the lens plane, we compute the deflection angle by summing the contributions from the cluster itself and the galaxy haloes.

We first apply two axially symmetric models, namely spheres with the NFW or the singular isothermal density profile. Second, we also apply the pseudo-elliptical NFW lens model in order to account for the possible elongation of the matter distribution of the cD galaxy. cD galaxies typically appear to be of elliptical shape, with isophotal axis ratios $b/a \sim 0.8$ (Porter et al., 1991). Moreover, the orientation of the brightest cluster ellipticals is usually not random, but correlates well with that of their host cluster. Asymmetries in the lensing matter distribution are known to improve the ability of the cluster to produce long and thin arcs. We also expect that the impact of a cD galaxy described by an elliptical model is largest when its orientation is aligned with the elongation direction of the host galaxy cluster. In the case of different orientations, the cD galaxy tends to circularize the mass distribution of the cluster in its central region. In order to quantify this effect, we carry out two sets of simulations; in the first, we randomly choose the orientation of the cD galaxy inside the cluster, while in the second the orientation is chosen such that the directions of the major and minor axes of the galaxy align with the major and minor eigenvalues of the cluster's deflection angle field, respectively. The galaxy ellipticity is assumed to be $e = 0.2$.

In Fig. 3, we show the relative change of the lensing cross sections for arcs with length-to-width ratio $L/W \geq 7.5$ as a function of the cluster virial mass for the simulations in Λ CDM and OCDM models. The lens redshift is $z_L = 0.27$, while sources are placed at $z_S = 1$. In each panel, we plot the results for all four models used to describe the cD galaxy. Both panels refer to simulations in which the virial mass of the cD galaxy is $5 \times 10^{13} h^{-1} M_\odot$.

As expected, the largest variations of the cross sections are typically found if the cD galaxy is modeled as a pseudo-elliptical NFW model whose orientation is aligned with that of the host cluster. On the other hand, cD galaxies with SIS profiles change the ability of the numerical clusters for producing long and thin arcs only by a very small amount.

In the Λ CDM model, a cD galaxy with mass $M_{cD} = 5 \times 10^{13} h^{-1} M_\odot$ changes the lensing cross section by a maximum amount between 60% and 200%, depending on the total cluster mass. The impact of the cD is generally larger in the less massive clusters. Of course, less massive cD galaxies have smaller impact on the lensing cross sections: in more realistic cases of cD galaxies with

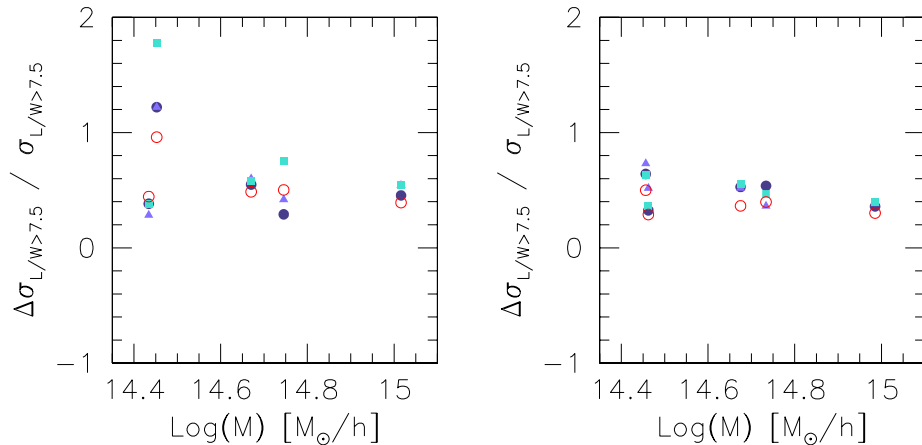


Figure 3. Relative change in the cross sections for arcs with length-to-width ratios exceeding 7.5 as a function of cluster mass for the numerically simulated clusters in the Λ CDM (left panel) and OCDM models. Filled circles, triangles and squares mark the results obtained modeling the cD as an NFW sphere, a pseudo-elliptical NFW model with random orientation, and aligned with the orientation of the host cluster, respectively; open circles show the results found modeling the cD galaxy as a SIS. The mass of the cD galaxy is $5 \times 10^{13} h^{-1} M_{\odot}$.

mass $M_{\text{cD}} \lesssim 10^{13} h^{-1} M_{\odot}$, tangential-arc cross sections are increased by not more than $\sim 50\%$.

A similar trend is found in the OCDM model, but the variations of the cross sections are smaller in this case. For example, in the simulations with the most massive cDs, the cross sections change by approximately 40% – 80% only. This behavior was expected because the clusters in the OCDM model are generally more compact compared than those in the Λ CDM model. Including the cD, the mass in the very central part of the clusters changes less compared to the clusters in the Λ CDM model. Cross sections for arcs with different minimal length-to-width ratios show similar variations.

We thus conclude from our conservative estimates of the impact of cD galaxies on strong-lensing cross sections by galaxy clusters that they may increase the arc-formation probability by perhaps up to $\sim 50\%$ in realistic situations, but certainly by far not enough for explaining the discrepancy between simulations in Λ CDM models and the observed abundance of arcs.

3.2. The impact of mergers on arc statistics

We investigate an other possible effect which could not be properly considered in the previously mentioned numerical simulations of gravitational lensing by galaxy clusters. In those works, the lensing cross sections for giant arcs of each numerical model were evaluated at different redshifts, with a typical time separation between two consecutive simulation outputs of approximately $\Delta t \sim 1$ Gyr. Therefore all the dynamical processes arising in the lenses on time scales smaller than Δt were not resolved.

N-body simulations show that dark matter haloes of different masses continuously fall onto rich clusters of galaxies (Tormen, 1997). The typical time scale for such events is $\sim 1 \div 2$ Gyr, which therefore might be too short for having been properly taken into account in the previous lensing simulations.

Given the strong impact of substructures on the lensing properties of galaxy clusters, it is reasonable to expect that during the passage of a massive mass concentration through or near the cluster center, the lensing efficiency might sensitively fluctuate. Indeed, when the substructure is approaching the main cluster clump, the intensity of the shear field and, consequently, the shape of the critical curves might substantially change. Moreover, while the infalling dark matter halo gets closer the cluster center, the projected surface density increases, making the cluster much more efficient for strong lensing.

We use the ray-tracing technique for studying the lensing properties of a numerically simulated galaxy clusters while a mass concentration orbit very close to the cluster center. In particular, we investigate an “optimal” projection of this cluster, where a substructure is seen to pass exactly through the center of main cluster clump.

The numerical model we study here is part of a set of 17 objects obtained using the technique of re-simulating at higher resolution a patch of a pre-existing cosmological simulation. The re-simulation method is described in Tormen et al. (1997). A detailed discussion of the dynamical properties of the whole sample of these simulated clusters is presented elsewhere (Tormen, Moscardini & Yoshida 2003, in preparation). A major merger occurs in this cluster between redshifts $z = 0.25$ and $z = 0.15$. At redshift $z \sim 0.25$, when their virial regions merge, the main cluster clump and the infalling substructure have virial masses of $\sim 7 \times 10^{14} h^{-1} M_{\odot}$ and $\sim 3 \times 10^{14} h^{-1} M_{\odot}$, respectively. In order to have a very good time resolution to resolve in detail all the merging phases, we decided to re-simulate the cluster between $z = 0.25$ and $z = 0.15$, obtaining 101 equispaced outputs which we use for our following lensing analysis.

As expected, the critical lines of the numerical lens evolve strongly during the merger event. We show the critical lines at some relevant redshifts in Fig. (4). At redshift $z = 0.230$, the main cluster clump and the infalling substructure develop separate critical lines. The largest mass concentration also produces a small radial critical line (enclosed by the more extended tangential critical line). While the merger proceeds, the tangential critical lines are stretched towards each other. This is due to the increasing shear in the region between the mass concentrations. The critical lines merge approximately at redshift $z = 0.214$. After that, there exists a single critical line, which, after a short phase of shrinking, expands isotropically while the two clumps overlap. The isotropic expansion is due to the increasing convergence due to the larger amount of matter concentrated at the cluster center. This happens at $z \sim 0.203$. When the substructure moves to the opposite side, the tangential critical line stretches again and reaches its maximum elongation at $z \sim 0.190$. Then, separate critical lines appear around each clump. Their size decreases for $z \rightarrow 0$ because both the shear and the convergence between the two mass concentration decrease as their distance grows.

The lensing cross sections for long and thin arcs change during the merger accordingly to the evolution of the critical lines. As an example, the cross section

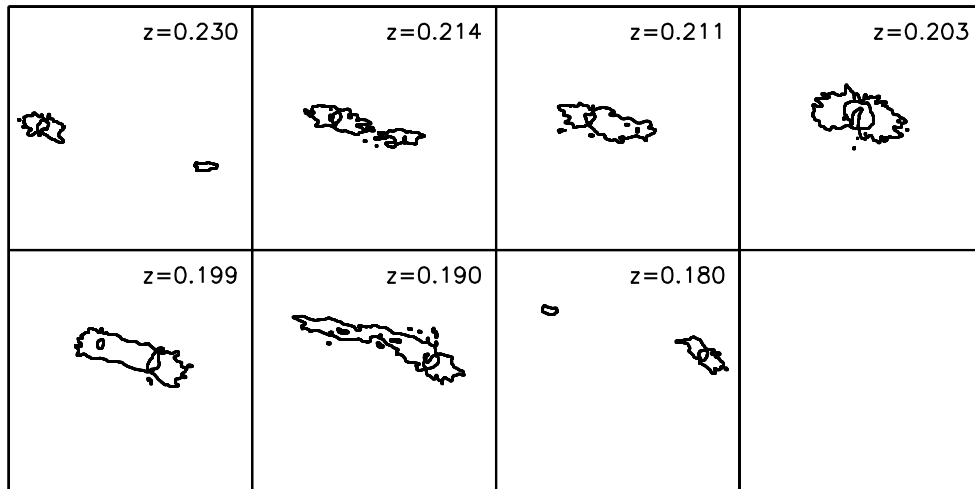


Figure 4. Critical lines of the numerically simulated galaxy cluster at the several redshifts between $z = 0.230$ and $z = 0.180$, during the merging phase. The scale of each panel is $375''$.

for arcs with $L/W \geq 7.5$ as function of redshift is shown in Fig. (5). The cross section grows by a factor of two between $z \sim 0.240$ and $z \sim 0.220$. Then, it further increases by a factor of five between $z \sim 0.220$ and $z \sim 0.200$, i.e. within ~ 0.2 Gyr. The curves have three peaks, located at redshifts $z_1 = 0.214$, $z_2 = 0.203$ and $z_3 = 0.190$. The peaks at z_1 and z_3 correspond to the maximum extent of critical curves along the merging direction *before* and *after* the moment when the merging clumps overlap; the peak at z_2 occurs when the distance of the infalling substructure from the merging clump is minimum. Two local minima arise between the three maxima at redshifts $z_4 = 0.211$ and $z_5 = 0.199$, where the cross sections are a factor of two smaller than at the peaks. At these redshifts, the critical lines have shrunk along the merging direction. The cross section reduces by more than one order of magnitude after $z = 0.190$.

Therefore, during the merger, our simulated cluster becomes extremely more efficient to produce tangential arcs. The infalling substructure starts affecting the cross sections for long and thin arcs when its distance from the main cluster clump is approximately equivalent to the cluster virial radius ($\sim 1.5 h^{-1}\text{Mpc}$), and the largest effects are seen at three different times: 1) when the critical lines (and the corresponding caustics) merge, i.e. when the shear between the mass concentrations is sufficient to produce the largest elongation of the critical lines along the direction of merging. This happens ~ 100 Myr before and after the substructure crosses the cluster center; 2) when the two clumps overlap, i.e. when the projected surface density or convergence is maximal, producing the largest *isotropic* expansion of critical lines and caustics.

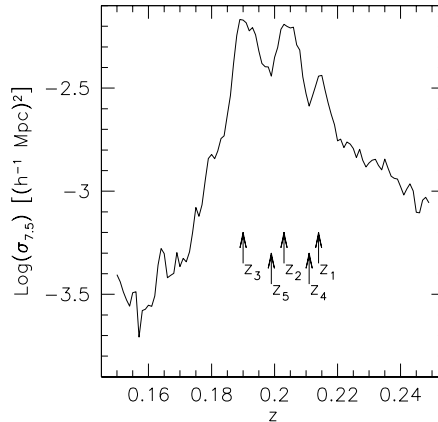


Figure 5. Lensing cross section for arcs with $L/W > 7.5$ as function of redshift.

Therefore, our results show that cluster mergers could play an important role for arc statistics. In particular, since the lensing efficiency grows by one order of magnitude during mergers, they might be the solution of the *arc statistics problem*.

It is quite important to notice that mergers might have some other important observational implications to account for. In fact the largest sample of clusters used for arc statistics studies (Luppino et al, 1999) was selected in the X-ray band, where the luminosity is due to bremsstrahlung emission. This is very sensitive to the dynamical processes arising in the cluster, since it is proportional to the square gas density. Therefore, we expect that the cluster X-ray luminosity has large variations during a merging phase.

By using a code for simulating observations in the X-ray band by the *Chandra* satellite (Gardini et al., 2003, in preparation), we measure the observed X-ray luminosity of our numerical cluster at several times during the merging phase. In Fig. (6) we show the observed X-ray luminosity as function of redshift. The curve has a narrow and almost symmetric peak located at $z \sim 0.200$. The X-ray luminosity grows by more than a factor of four between $z \sim 0.300$ and $z \sim 0.200$, by roughly a factor of ~ 2.5 between $z \sim 0.230$ and $z \sim 0.200$ and by roughly a factor of ~ 1.55 between $z \sim 0.210$ and $z \sim 0.200$. The width at half maximum of the peak is approximately $\Delta z \lesssim 0.05$.

If a cluster sample is built by collecting all the objects with X-ray luminosity L_X larger than a given minimum threshold, we expect that many merging clusters are present among them, since they are stronger X-ray emitters. Since these are all very efficient clusters for producing gravitational arcs, this could introduce a bias in the observationally determined frequency of *giant arc*, which could become so large with respect to what predicted by previous numerical lensing simulations in Λ CDM model. However, it is quite difficult to make more robust conclusions here since only one cluster has been analyzed. Further investigations are needed on this subject. In any case, our results show that much

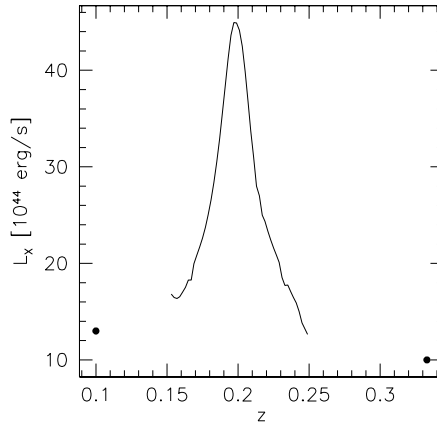


Figure 6. X-ray luminosity L_x of the numerically simulated cluster as function of redshift. The curve is accurately sampled in the redshift range $z = 0.15 \div 0.25$. The X-ray luminosity has been measured also at $z = 0.1$ and $z = 0.333$, where is indicated by the filled circles.

caution must be used when selecting clusters for arc statistics studies through their X-ray emission.

4. Conclusions

In the first part of this paper, we discussed the analytic and numerical methods used in arc statistics studies. We showed that both axially symmetric and elliptical analytic models fail to reproduce the efficiency for producing long and thin arcs of numerically simulated galaxy clusters. The deviations of the numerical lensing cross sections from their analytical approximations can be attributed to substructures inside clusters and tidal fields contributed by the cluster surroundings, effects which cannot reasonably and reliably be mimicked in analytic models. On the basis of these results, we conclude that, in order to derive precise constraints on cosmology or cluster structure and evolution, realistic cluster lens models are required, for which numerical simulations seems to be the only reliable choice.

In the second part, we discussed two recent extensions of the numerical lensing simulations. First, we investigate the effects of cD galaxies on the cluster efficiency for long and thin arcs. We found that reasonably massive cD galaxies at the cluster center may increase the arc-formation probability by perhaps up to $\sim 50\%$. Second, we study the impact of major mergers on arc statistics. By measuring with high time resolution the cross sections for long and thin arcs of a numerical cluster model during a merger phase, we verified that the cluster ability of producing tangential arcs may grow by one order of magnitude while such events occur. This result is particularly important because it confirms that mergers in clusters might play a very important role in arc statistics. In particular they might be a possible solution to the well know arc statistics problem.

References

- Bartelmann M., 1996, *A&A*, 313, 697
- Bartelmann M., Huss A., Colberg J. M., Jenkins A., Pearce F. R., 1998, *A&A*, 330, 1
- Bartelmann M., Meneghetti M., Perrotta F., Baccigalupi C., Moscardini L., 2003b, preprint, astro-ph/0210066
- Bartelmann M. Perrotta F., Baccigalupi C., 2003a, *A&A*, 396, 21
- Bennett C.L., Halpern M., Hinshaw G., Jarosik N., Kogut A., Limon M., Meyer S.S., Page L., Spergel D.N., Tucker G.S., Wollack E., Wright E.L., Barnes C., Greason M.R., Hill R.S., Komatsu E., Nolte M.R., Odegard N., Peirs H.V., Verde L., Weiland J.L., 2003, preprint, astro-ph/0302207
- Cooray A. R., Quashnock J. M., Miller M. C., 1999, *ApJ*, 511, 562
- de Bernardis P., Ade P. A. R., Bock J. J., et al., 2002, *ApJ*, 564, 559
- Gladders M.D., Hoekstra H., Yee H.K.C., Hall P.B., Barrientos L.F., 2003, preprint, astro-ph/0303341
- Golse G., Kneib J.-P., 2002, *A&A*, 387, 788
- Kassiola A., Kovner I., 1993, *ApJ*, 417, 450
- Kauffmann G.A.M., Colberg J.M., Diaferio A., White S.D.M., 1999, *MNRAS*, 303, 188
- Kaufmann R., Straumann N., 2000, *Ann. Phys.*, 11, 507
- Kormann R., Schneider P., Bartelmann M., 1994, *A&A*, 284, 285
- Li L.-X., Ostriker J.P., 2002, *ApJ*, 566, 652
- Luppino G. A., Gioia I. M., Hammer F., Le Fèvre O., Annis J. A., 1999, *A&AS*, 136, 137
- Meneghetti M., Bartelmann M., Moscardini L., 2003a, *MNRAS*, 340, 105
- Meneghetti M., Bartelmann M., Moscardini L., 2003b, preprint, astro-ph/0302603
- Meneghetti M., Bolzonella M., Bartelmann M., Moscardini L., Tormen G., 2000, *MNRAS*, 314, 338
- Meneghetti M., Yoshida N., Bartelmann M., Moscardini L., Springel V., Tormen G., White S.D.M., 2001, *MNRAS*, 325, 435
- Navarro J.F., Frenk C.S., White S.D.M., 1997, *ApJ*, 490, 493
- Perlmutter S., 1998, *AAS*, 30, 1388
- Perrotta F., Baccigalupi C., Bartelmann M., de Zotti G., Granato G.L., 2002, *MNRAS*, 329, 445
- Porter A. C., Schneider D. P., Hoessel J. G., 1991, *AJ*, 101, 1561
- Tormen G., 1997, *MNRAS*, 290, 411
- Tormen G., Bouchet F., White S.D.M., 1997, *MNRAS*, 286, 865
- Wright C.O., Brainerd T.G., 2000, *ApJ*, 534, 34
- Wu X., Hammer F., 1993, *MNRAS*, 262, 187
- Wyithe J.S.B., Turner E.L., Spergel D.N., 2001, *ApJ*, 555, 504
- Zaritsky D., Gonzalez A. H., 2003, *ApJ*, 2003, 584, 691